

## Letter

**Discovery of a potent, selective, and orally available  
PI3Kd inhibitor for the treatment of inflammatory diseases**

Montse Erra, Joan Taltavull, Angelique Gréco, Francisco Javier Bernal, Juan Francisco Caturla, Jordi Gracia, María Domínguez, Mar Sabaté, Stéphane Paris, Salomé Soria, Begoña Hernández, Clara Armengol, Judit Cabedo, Mònica Bravo, Elena Calama, Montserrat Miralpeix, and Martin D. Lehner

ACS Med. Chem. Lett., **Just Accepted Manuscript** • DOI: 10.1021/acsmedchemlett.6b00438 • Publication Date (Web): 30 Nov 2016

Downloaded from <http://pubs.acs.org> on November 30, 2016

**Just Accepted**

"Just Accepted" manuscripts have been peer-reviewed and accepted for publication. They are posted online prior to technical editing, formatting for publication and author proofing. The American Chemical Society provides "Just Accepted" as a free service to the research community to expedite the dissemination of scientific material as soon as possible after acceptance. "Just Accepted" manuscripts appear in full in PDF format accompanied by an HTML abstract. "Just Accepted" manuscripts have been fully peer reviewed, but should not be considered the official version of record. They are accessible to all readers and citable by the Digital Object Identifier (DOI®). "Just Accepted" is an optional service offered to authors. Therefore, the "Just Accepted" Web site may not include all articles that will be published in the journal. After a manuscript is technically edited and formatted, it will be removed from the "Just Accepted" Web site and published as an ASAP article. Note that technical editing may introduce minor changes to the manuscript text and/or graphics which could affect content, and all legal disclaimers and ethical guidelines that apply to the journal pertain. ACS cannot be held responsible for errors or consequences arising from the use of information contained in these "Just Accepted" manuscripts.



# Discovery of a potent, selective, and orally available PI3K $\delta$ inhibitor (LAS191954) for the treatment of inflammatory diseases.

Montse Erra<sup>‡\*</sup>, Joan Taltavull<sup>‡</sup>, Angelique Gréco<sup>‡€</sup>, Francisco Javier Bernal<sup>‡</sup>, Juan Francisco Caturla<sup>‡</sup>, Jordi Gràcia<sup>‡</sup>, María Domínguez<sup>‡</sup>, Mar Sabaté<sup>‡</sup>, Stéphane Paris<sup>‡</sup>, Salomé Soria<sup>‡</sup>, Begoña Hernández<sup>‡□</sup>, Clara Armengol<sup>#</sup>, Judit Cabedo<sup>Δ</sup>, Mónica Bravo<sup>Δ</sup>, Elena Calama<sup>Δ</sup>, Montserrat Miralpeix<sup>Δ</sup>, and Martin D. Lehner<sup>Δ‡</sup>.

<sup>‡</sup>Medicinal Chemistry and Screening, <sup>€</sup>Pharmacokinetics and Metabolism, <sup>#</sup>Systems Biology, <sup>Δ</sup>Respiratory Therapeutic Area, Almirall R&D, Barcelona, Spain.

**KEYWORDS:** Phosphoinositide-3-kinase delta inhibitor, PI3K $\delta$  inhibitor, structure-activity relationship, autoimmune diseases, inflammatory diseases, lead optimization.

**ABSTRACT:** The delta isoform of the Phosphatidylinositol 3-kinase (PI3K $\delta$ ) has been shown to have an essential role in specific immune cell functions and thus represents a potential therapeutic target for autoimmune and inflammatory diseases. Herein, the optimization of a series of pyrrolotriazinones as potent and selective PI3K $\delta$  inhibitors is described. The main challenge of the optimization process was to identify an orally available compound with a good pharmacokinetic profile in pre-clinical species that predicted a suitable dosing regimen in humans. Structure-activity relationships and structure-property relationships are discussed. This medicinal chemistry exercise led the identification of LAS191954 as a candidate for clinical development.

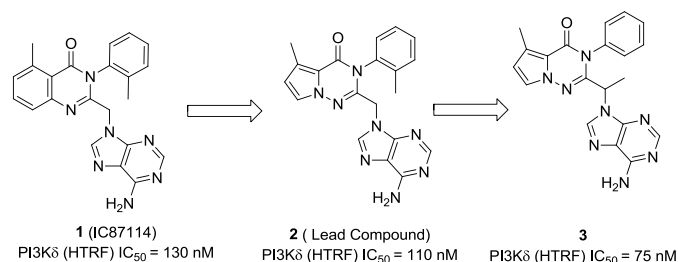
The phosphatidylinositol-3-kinase (PI3K) signal transduction pathway is central to a plethora of different cellular processes involving metabolism, proliferation, differentiation or activation. Hence, manipulation of the PI3K pathway represents an interesting approach for treatment of a number of different pathological conditions such as cancer, where inhibitors of class IA PI3K with varying isoform selectivity profiles have already been established as treatment options for different indications.

In the immune system, the PI3K delta isoform plays a central role in both innate and adaptive immune cell functions. Taking advantage of the strong dependency of B cells on functional PI3K $\delta$ <sup>1</sup>, the oral PI3K $\delta$  inhibitor Idelalisib has been successfully developed as a novel treatment for different types of B-cell malignancies<sup>2</sup>. In addition, the involvement of PI3K $\delta$  in central immune functions suggests a therapeutic potential of PI3K $\delta$  inhibitors as novel broad-acting anti-inflammatory agents for autoimmune diseases<sup>3</sup> and pathologies with an allergic or inflammatory component such as allergic rhinitis<sup>4</sup>, asthma<sup>5</sup>, or COPD<sup>6</sup>. Apart from inhibiting B cell activation, pharmacological inhibition of PI3K delta has been demonstrated to attenuate T cell receptor induced cytokine production<sup>7</sup>, degranulation of basophils and mast cells<sup>4,8</sup> as well as induction of oxidative burst by neutrophils<sup>9</sup>. In addition, PI3K $\delta$  seems to be involved in corticosteroid resistance induced by oxidative stress in macrophages<sup>10</sup>, thus indicating an activity profile complementary to other currently treatments such as corticosteroids.

The discovery of the propeller-shaped inhibitor **1** (IC87114, ICOS) and the mechanisms by which  $\delta$  isoform selectivity can be accomplished focused our attention<sup>11</sup>. Following this strategy, our efforts toward the identification of new PI3K $\delta$  inhibitors were based on a pyrrolotriazinone scaffold as shown in

Scheme 1. Our initial lead **2** showed similar PI3K $\delta$  inhibitor potency to IC87114 (110 nM versus 130 nM) and also high selectivity against the other class I PI3K isoforms. Moving the methyl group from the phenyl ring in compound **2** to the linker (compound **3**), slightly improved the PI3K $\delta$  inhibitor potency to 75 nM and removed the potential for atropisomerism<sup>12</sup> present in ortho-substituted compounds **1** and **2**. Taking into account the stereochemistry of known PI3K $\delta$  selective inhibitors in the clinic such as Idelalisib<sup>13</sup> and Duvelisib<sup>14</sup>, the S-enantiomers were initially targeted.

**Scheme 1. Pyrrolotriazinone scaffold**

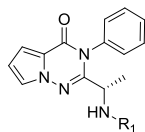


Thus, an extensive structure-activity relationship (SAR) study was then performed around compound **3** to improve the potency and modulate ADME properties.

Initially, an exploration of the hinge binder region was undertaken and PI3K $\delta$  inhibitory potency in both enzymatic and cellular assays was assessed together with *in vitro* metabolism<sup>15</sup> for each compound (Table 1). Introduction of other purine-like hinge binders (**4**, **5**) increased the *in vitro* potency for PI3K $\delta$  considerably and the compounds showed low *in vitro* metabolism. Other bicyclic rings (**6-8**) demonstrated lower potency and decreased metabolic stability when com-

pared to compounds **4** and **5**. Monocyclic rings were then studied and cyanopyrimidine **11** showed the best overall balance between potency and *in vitro* metabolism.

**Table 1. SAR exploration of the hinge binder**



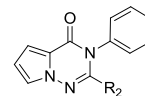
Compd	R <sub>1</sub>	PI3Kδ (HTRF) <sup>a</sup> IC <sub>50</sub> (nM)	M-CSF p-Akt <sup>b</sup> IC <sub>50</sub> (nM)	% Metabo- lism (rat/human) <sup>c</sup>
4		10	7	18 / 30
5		3.1	6.5	30 / 26
6		60	-	100 / 86
7		52	150	44 / 49
8		9	47	48 / 58
9		73	210	-
10		12	-	51 / 43
11		4.3	4.7	15 / 24
12		91	76	25 / 33
13		1200	-	-

<sup>a</sup>PI3Kδ activities were measured with an ATP concentration fixed at the Km of PI3Kδ by HTRF, where the PIP3 product is detected by displacement of biotin-PIP3 from an energy transfer complex. <sup>b</sup>THP-1 cells were treated with compounds for 30 min., stimulated with M-CSF at EC<sub>80</sub> for 3 minutes and then lysed to measure (by ELISA) pAkt (Thr308) produced through PI3Kδ. <sup>c</sup>% metabolism expressed as disappearance of parent compound after microsomal incubation for 30 min (1 mg/ml protein and 5 μM compound at 37 °C).

Optimization of the linker was then explored as shown in Table 2. An ethyl group was well tolerated giving a compound (**14**) of similar potency to the methyl derivative **4** but poorer microsomal stability. The corresponding (R)-enantiomer of **14** was synthesized (compound **15**) and the resultant drop off in potency confirmed the preference of PI3Kδ for the (S)-enantiomer. Replacing the hinge binder of compound **14** for the cyanopyrimidine (**16**) slightly improved potency and *in vitro* metabolism. Appending a hydroxyl group onto compounds **11**

and **16** resulted in derivative **18** and **17** respectively, but only compound **17** showed an improved microsomal stability whilst maintaining good PI3Kδ potency. In contrast, introduction of a trifluoroethyl group (compound **19**) was less tolerated. Cyclic analogue **20** kept *in vitro* potency but was metabolically less stable. Introduction of fluorine atoms in the cyclopentyl ring of **20** with the aim of increasing metabolic stability led to a less potent compound **21**. Introduction of a spirocyclic ring was also studied (compound **22**) but a big drop off in potency was observed.

**Table 2. Linker SAR exploration**



Compd	R <sub>2</sub>	PI3Kδ (HTRF) <sup>a</sup> IC <sub>50</sub> (nM)	M-CSF p-Akt <sup>b</sup> IC <sub>50</sub> (nM)	% Metabo- lism (rat/human) <sup>c</sup>
14		25	-	38 / 49
15		1800	-	32 / 30
16		11	18	32 / 32
17		4.8	16	ND / 7
18		13	51	24 / 31
19		610	1600	-
20		4.6	6.6	46 / 48
21		31	370	30 / 35
22		3400	-	-

<sup>a</sup>PI3Kδ activities were measured with an ATP concentration fixed at the Km of PI3Kδ by HTRF, where the PIP3 product is detected by displacement of biotin-PIP3 from an energy transfer complex. <sup>b</sup>THP-1 cells were treated with compounds for 30 min., stimulated with M-CSF at EC<sub>80</sub> for 3 minutes and then lysed to measure (by ELISA) pAkt (Thr308) produced through PI3Kδ. <sup>c</sup>% metabolism expressed as

disappearance of parent compound after microsomal incubation for 30min (1 mg/ml protein and 5  $\mu$ M compound at 37  $^{\circ}$ C).

Compounds **11** and **17** were then profiled in a rat *in vivo* pharmacokinetic (PK) experiment. However, for both compounds, *in vivo* clearance in rat was higher than expected from the microsomal stability data, resulting in moderate systemic exposure and short half-lives (Table 3).

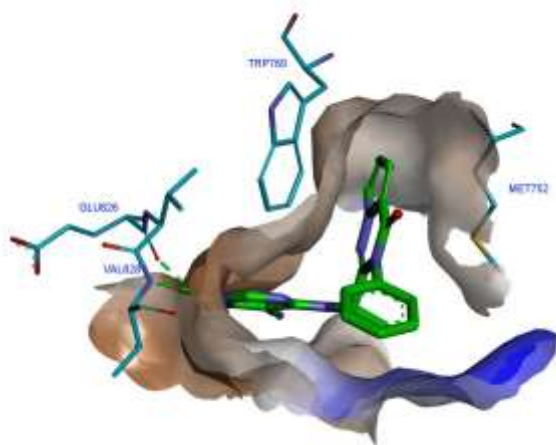
**Table 3. Rat PK profiles of compounds 11 and 17**

Compd	$t_{1/2}$ (h) <sup>a</sup>	AUC (ng*h/ml) <sup>a</sup>	Cl (ml/min/kg) <sup>a</sup>	Vss (l/kg) <sup>a</sup>
11	0.9	386	43.5	1.9
17	1.1	450	36.8	1.6

<sup>a</sup>Mean values (n=2) in Wistar rat after an administration of 1mg/kg i.v.. Parameters calculated from plasma samples:  $t_{1/2}$  = half-life, Cl = clearance, AUC = area under the curve, Vss = volume of distribution at steady state.

To better understand the binding mode of the ligands an X-ray co-crystal of human PI3K $\delta$  in complex with compound **11** was performed. The structure was solved at a resolution of 2.85Å, revealing the detailed binding mode of the ligand. Like IC87114, compound **11** adopted a propeller-shaped conformation where the pyrrolotriazinone moiety was sandwiched into the induced hydrophobic specificity pocket between Trp760 and Met752. The cyanopyrimidine ring of **11** served as the hinge binder and formed two specific hydrogen bonds to the main chain atoms of Val828 and Glu826. The following residues were found in the vicinity of the ligand with a maximum distance of 3.9Å: Met752, Pro758, Trp 760, Ile777, Tyr813, Ile825, Glu826, Val827, Val828, Ser831, Asp832, Met900, Ile910, and Asp911. A closer look at the binding pocket surface (Figure 1) suggested that the pyrrolotriazinone core ring could be substituted at the 5,6 or 7-position to further modulate potency.

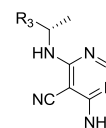
**Figure 1. X-ray co-crystal structure of the binding pocket surface of human PI3K $\delta$  containing compound 11**



Thus, several analogues with different substitutions on the pyrrolo ring were synthesized and tested. A methyl group was well tolerated in different positions (compounds **23** and **29**) but the resultant derivatives were metabolically unstable.

Appending a hydroxyl group onto the methyl group of **23** resulted in a compound **24** with reasonable PI3K $\delta$  inhibitor potency and improved metabolic stability. After further study it was found that placement of other substituents at position 5 (**25**, **26** and **27**) gave rise to compounds with excellent potencies and good metabolic stability. Further characterization of compound **25** showed the formation of GSH adducts following incubation of **25** with microsomes in presence of glutathione (GSH) and as such was not further profiled. Finally, the imidazotriazinone **32** showed a substantially diminished PI3K $\delta$  inhibitor potency in comparison to the corresponding pyrrolotriazinone **11**.

**Table 4. Distal core SAR exploration**



Compd	R <sub>3</sub>	PI3K $\delta$ (HTRF) <sup>a</sup> IC <sub>50</sub> (nM)	M-CSF p-Akt <sup>b</sup> IC <sub>50</sub> (nM)	% Metabolism (rat/human) <sup>c</sup>
23		1.1	1.6	44 / 80
24		4.3	35	7 / 23
25		1.1	3.8	9 / 13
26 LAS191954		2.6	7.8	20 / 16
27		3.0	3.0	16 / 37
28		17	51	23 / 34
29		8.8	11	54 / 82
30		4.0	11	24 / 22
31		71	380	-
32		57	210	14 / 23

<sup>a</sup>PI3K $\delta$  activities were measured with an ATP concentration fixed at the Km of PI3K $\delta$  by HTRF, where the PIP<sub>3</sub> product is detected by displacement of biotin-PIP<sub>3</sub> from an energy transfer complex. <sup>b</sup>THP-1 cells were treated with compounds for 30 min., stimulated with M-CSF at EC<sub>80</sub> for 3 minutes and then lysed to measure (by ELISA) pAkt (Thr308) produced through PI3K $\delta$ . <sup>c</sup>% metabolism expressed as disappearance of parent compound after microsomal incubation for 30 min (1 mg/ml protein and 5  $\mu$ M compound at 37  $^{\circ}$ C).

From this set of compounds, **26** and **27** were further profiled in a rat *in vivo* PK experiment (Table 5) to determine if the *in vitro* metabolism results were, in these cases, predictive of the *in vivo* clearance values. These results were compared with Idelalisib, the most advanced compound in clinical development at that moment.

**Table 5. Rat PK profiles of compounds 26 and 27 in comparison with Idelalisib**

Compd	t <sub>1/2</sub> (h) <sup>a</sup>	AUC (ng·h/ml) <sup>a</sup>	Cl (ml/min/kg) <sup>a</sup>	V <sub>z</sub> (l/kg) <sup>a</sup>	F (%) <sup>b</sup>
Idelalisib	0.8	512	32.8	2.2	68
26	3.1	1729	9.6	2.6	101
27	3.3	2040	8.6	2.4	113

<sup>a</sup>Mean values (n=2) in Wistar rat after an administration of 1mg/kg i.v. <sup>b</sup>Mean values (n=2) in Wistar rat after an administration of 1mg/kg p.o.

As seen in Table 5, compounds **26** and **27**, with substituents at position 5 of the pyrrolo ring, showed increased plasma exposure compared to unsubstituted compounds **11** and **17**, excellent oral bioavailability and reduced clearance in rat, which was more consistent with the observed microsomal stability values.

Additionally, the PK properties of both compounds **26** and **27** were studied in dog as a second preclinical species to allow for prediction of the probable posology in humans based on allometric scaling. The dog *in vivo* PK data are shown in Table 6. Both compounds **26** and **27** displayed a superior PK profile to Idelalisib in the two preclinical species. Compound **26** (LAS191954), with excellent oral bioavailability and low clearance in the two species, gave a superior predicted half-life in humans and was further profiled.

**Table 6. Dog PK profiles of compounds 26 and 27 in comparison with Idelalisib**

Compd	t <sub>1/2</sub> (h) <sup>a</sup>	AUC (ng·h/ml) <sup>a</sup>	Cl (ml/min/kg) <sup>a</sup>	V <sub>z</sub> (l/kg) <sup>a</sup>	F (%) <sup>b</sup>
Idelalisib	1.6	924	21.5	2.5	-
26	10.2	9441	1.4	1.2	98
27	4.2	3937	4.2	1.5	-

<sup>a</sup>Mean values (n=2) in Beagle dog after an administration of 1mg/kg i.v. <sup>b</sup>Mean values (n=3) in Beagle dog after an administration of 1mg/kg p.o.

For the assessment of selectivity, the enzymatic potency of compound **26** on the four class I PI3K recombinant human isoforms was determined by HTRF with a compound preincubation time of 30 min. Compound **26** showed a potency on the target of 2.6 nM, with the highest selectivity versus PI3K $\alpha$  (8.2  $\mu$ M) and the lowest versus PI3K $\gamma$  and PI3K $\beta$  (72 and 94 nM respectively). The compound was then tested in a

primary PI3K $\delta$ -dependent cellular assay based on M-CSF-induced AKT phosphorylation, a downstream effector of PI3K $\delta$ , in the human monocytic cell line THP-1. An IC<sub>50</sub> of 7.8 nM was obtained indicating that the compound had excellent permeability and cellular activity. To evaluate the cellular inhibition of PI3K $\beta$ , an assay based on stimulation of HUVEC cells with sphingosine-1-P was employed<sup>16</sup>. The results (IC<sub>50</sub> = 295 nM) indicated that the enzymatic selectivity between  $\delta$  and  $\beta$  isoforms (36-fold) was maintained at the cell-based level (38-fold). The compound was also selective against an extensive panel of protein and lipid kinases and GPCRs.

PI3K $\delta$  kinase is involved in the activation of B cells upon antigen binding to the B cell receptor (BCR)<sup>17</sup> and thus inhibitors of PI3K $\delta$  are expected to inhibit BCR activation. The effect of LAS191954 on the function of human B cells was assessed *in vitro* by crosslinking the B-cell receptor with anti-IgD antibodies and assessing the early activation marker CD69 in the CD19+ B cell subset by flow cytometry. On isolated PBMC, compound **26** showed an IC<sub>50</sub> of 4.6 nM. Similar assay performed in human whole blood yielded an IC<sub>50</sub> of 47 nM.

From an ADME perspective, further *in vitro* characterization of compound **26** was performed as summarized in Table 7. Plasma protein binding<sup>18</sup> was low in preclinical species (60–65% in mouse/rat/dog) in contrast to human (95%). Plasma protein binding may be the major factor accounting for the difference in potency between the isolated human PBMC and whole blood assays previously described. The compound showed a good PAMPA<sup>19</sup> value as expected by the cellular potencies obtained. Moreover, compound **26** did not present any signs of instability in plasma. The potential capacity of compound **26** to inhibit the main human CYP450 isoforms (CYP1A2, 3A4, 2D6, 2C9 and 2C19) was investigated in human liver microsomes. Compound **26** displayed IC<sub>50</sub> > 25  $\mu$ M for the five CYP isoforms assayed. No differences were observed after 15 min of preincubation time, suggesting that compound **26** is not a mechanism-based inhibitor. In addition, the potential capacity of the compound to induce CYP1A and 3A4 isoforms was assessed in cultured human cryopreserved hepatocytes and compound **26** did not increase neither CYP1A nor 3A4 activity at concentrations up to 50  $\mu$ M. Taking into account the results of these studies, drug-drug interactions due to induction or inhibition of human CYP450 isoforms are not expected in a clinical setting. Furthermore, no formation of GSH-adducts was observed following incubation of compound **26** with rat and human liver microsomes in the presence of glutathione (GSH).

**Table 7. In vitro ADME profile of compound 26**

Human PPB (% bound) <sup>a</sup>	PAMPA P <sub>app</sub> ( $\times 10^{-6}$ cm/s) <sup>b</sup>	Plasma stability (24h) <sup>c</sup>	CYP450 inhibition <sup>d</sup>
95.4	2.8	100%	> 25 $\mu$ M

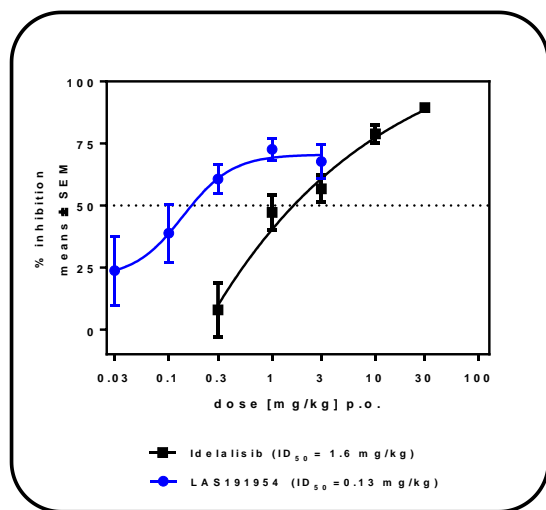
<sup>a</sup>Mean PPB values determined by equilibrium dialysis at a plasma concentration of 1  $\mu$ M at 37°C. <sup>b</sup>Permeability values at RT in PBS (containing 2% DMSO), compound concentration in donor compartment: 20  $\mu$ M. <sup>c</sup>Compound **26** stability at 37°C at 2  $\mu$ g/ml in plasma (anticoagulant: sodium heparin) <sup>d</sup>CYP450 in HLM with and without preincubation for CYP1A2, 3A4, 2D6, 2C9 and 2C19 isoforms.

In terms of cardiac safety, compound **26** did not show any activity on the hERG channel up to 10  $\mu$ M.

As a consequence of these encouraging results, the compound was further characterized in different *in vivo* models.

PI3K $\delta$  has been implicated in T-cell proliferation *in vitro* and *in vivo*. Cytokine production induced by concanavalin A (con A) or anti-CD3 antibody activation of naïve CD4<sup>+</sup> T cells in mice is blocked by PI3K $\delta$  inhibition<sup>20</sup>. To assess the effect of LAS191954 on T cell cytokine production *in vivo*, a rat model of con A induced IL2 production was employed in which the compound was administered orally one hour prior to an intravenous con A challenge (10 mg/kg) and IL2 levels were measured 90 minutes later. LAS191954 inhibited IL2 production with an ID<sub>50</sub> of 0.13 mg/kg as compared to an ID<sub>50</sub> of 1.6 mg/kg of Idelalisib as shown in Figure 2.

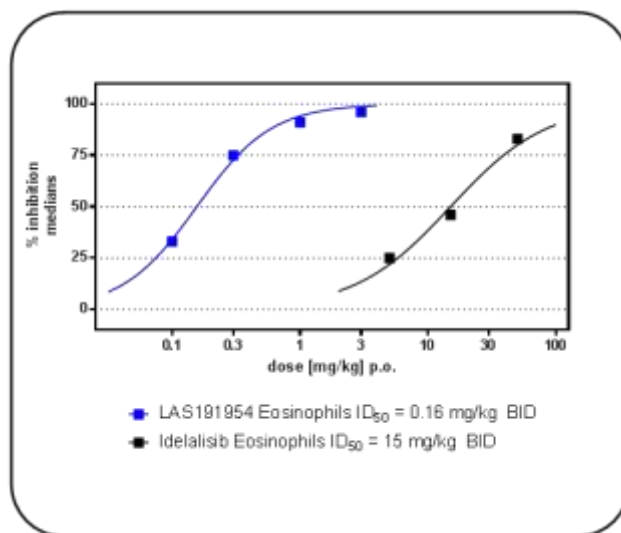
**Figure 2. Inhibition of ConA induced increase in IL-2 levels in rat plasma of LAS191954 vs reference compound Idelalisib**



PI3K $\delta$  participates in the proliferation, differentiation, migration and cytokine production of T lymphocytes; in the migration and release of ROS and proteases by neutrophils as well as in the migration, alternative M2 activation and loss of steroid sensitivity of macrophages. PI3K $\delta$  additionally regulates Fc $\epsilon$  mediated mast cell and basophil degranulation. Thus, the anti-inflammatory efficacy of LAS191954 was assessed in an airway allergic inflammation model characterized by infiltration of eosinophils to the alveolar compartment in response to ovalbumin challenge in previously sensitized Brown Norway rats.

A twice daily administration of LAS191954 1h prior to and 6h post ovalbumin (OVA) challenge dose-dependently reduced the number of eosinophils in the bronchoalveolar lavage (BAL) at 24h in rat with an ID<sub>50</sub> of 0.16 mg/kg. The reference compound Idelalisib, administered also twice daily, displayed a considerably lower potency with an ID<sub>50</sub> of 15 mg/kg.

**Figure 3. Inhibition of OVA BAL cell accumulation in BN rats at 24h by twice daily doses of LAS191954 and Idelalisib**



In both *in vivo* models LAS191954 showed efficacy at significantly lower doses than Idelalisib. These results could not be explained by differences in *in vitro* potency as Idelalisib exhibited a similar cellular PI3K $\delta$  inhibitor potency with an IC<sub>50</sub> of 7.6 nM, but they are in accordance with a superior PK profile (higher systemic exposure and longer half-life) of LAS191954 in rat.

In summary, a new series of potent and selective PI3K $\delta$  inhibitors has been identified. The SAR exercise focused on optimizing both the *in vitro* potency and the ADME profile of the compounds in order to find a potentially once-a-day drug. This culminated in the identification of LAS191954 as a candidate for clinical development.

## ASSOCIATED CONTENT

### Supporting Information

Characterization of all compounds. Experimental procedures for the sequence leading to key compound **26**. Description of all biological assays and *in vivo* studies. Crystallographic data collection and refinement statistics for crystal structure of compound **11**. This material is available free of charge via the Internet at <http://pubs.acs.org>.

### Accession Codes

PDB code for X-ray crystal structure described in this study has been deposited in the Protein Data Bank under the following accession codes: 5M6U (compound **11** in complex with PI3K $\delta$ )

## AUTHOR INFORMATION

### Corresponding Author

\* Phone: + 34 93 312 87 14. E-mail: [montse.erra@almirall.com](mailto:montse.erra@almirall.com)

### Author Contributions

The manuscript was written through contributions of all authors. All authors have given approval to the final version of the manuscript.



## Present Addresses

<sup>†</sup>Pharmaxis Ltd, 20 Rodborough Road, Frenchs Forest, NSW 2086, Australia

<sup>‡</sup>Bionorica SE, Kerschensteinerstraße 11-15, 92318 Neumarkt, Germany.

<sup>□</sup>Fundació ACE, Marqués de Sentmenat, 57, 08029 Barcelona, Spain.

## Notes

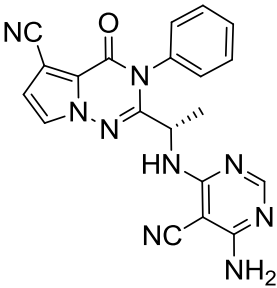
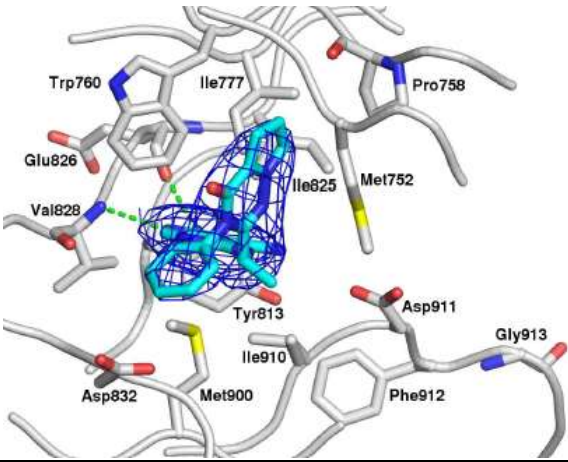
The authors declare no competing financial interest.

## ACKNOWLEDGMENT

The authors wish to thank Proteros Biostructures GmbH for X-ray structure determination of human PI3K $\delta$  in complex with compound **11** (PDB code: 5M6U). We also acknowledge the significant technical support provided by Jordi Sanahuja, Gaspar Casals and Antonia Molina. We thank Sonia Espinosa and Josep M. Huerta for their support on physicochemical properties analysis and structural characterization of compounds.

## REFERENCES

- Puri K. D.; Gold M.R. Selective inhibitors of phosphoinositide 3-kinase delta: modulators of B-cell function with potential for treating autoimmune inflammatory diseases and B-cell malignancies. *Front. Immunol.* **2012**, *3*, 256.
- Cheah, C. Y.; Fowler N. H. Idelalisib in the management of lymphoma. *Blood*, **2016**, *128* (3), 331-6.
- Durand C. A.; Richer, M. J.; Brenker, K.; Graves, M.; Shanina, I.; Choi, K.; Horwitz, M. S.; Puri, K. D.; Gold, M. R. Selective Pharmacological Inhibition of Phosphoinositide 3-Kinase p110delta Opposes the Progression of Autoimmune Diabetes in Non-Obese Diabetic (NOD) Mice. *Autoimmunity* **2013**, *46* (1), 62-73.
- Horak F.; Puri K. D.; Steiner B. H.; Holes L.; Xing G.; Ziegelmayer P.; Ziegelmayer R.; Lemell P.; Yu A. Randomized Phase 1 study of the phosphatidylinositol 3-kinase  $\delta$  inhibitor Idelalisib in patients with allergic rhinitis. *J Allergy Clin. Immunol.* **2016**, *137* (6): 1733-41
- Rowan W. C.; Smith J. L.; Affleck K.; Amour A. Targeting phosphoinositide 3-kinase  $\delta$  for allergic asthma. *Biochem. Soc. Trans.* **2012**, *40* (1), 240-5.
- Sriskanharajah S.; Hamblin N.; Worsley S.; Calver A. R.; Hessel E. M.; Amour A. Targeting phosphoinositide 3-kinase  $\delta$  for the treatment of respiratory diseases. *Ann. N Y Acad. Sci.* **2013**, *1280*, 35-9.
- Soond D. R.; Björge E.; Moltu K.; Dale V. Q.; Patton D. T.; Torgersen K. M.; Galleway F.; Twomey B.; Clark J.; Gaston J. S.; Taskén K.; Bunyard P.; Okkenhaug K. PI3K p110delta regulates T-cell cytokine production during primary and secondary immune responses in mice and humans. *Blood*, **2010**, *115* (11), 2203-2213.
- Ali K.; Camps M.; Pearce W. P.; Ji H.; Rückle T.; Kuehn N.; Pasquali C.; Chabert C.; Rommel C.; Vanhaesebroeck B. Isoform-Specific Functions of Phosphoinositide 3-Kinases: p110 $\delta$  Not p110 $\gamma$  Promotes Optimal Allergic Responses In Vivo. *J. Immunol.*, **2008**, *180* (4), 2538-2544.
- Fung-Leung W. P. Phosphoinositide 3-kinase delta (PI3K $\delta$ ) in leukocyte signaling and function. *Cell Signal.*, **2011**, *23* (4), 603-8.
- Marwick J.A.; Caramori G.; Casolari P.; Mazzoni F.; Kirkham P. A.; Adcock I. M.; Chung K. F.; Papi A. A role for phosphoinositol-3-kinase delta in the impairment of glucocorticoid responsiveness in patients with chronic obstructive pulmonary disease. *J. Allergy Clin. Immunol.*, **2010**, *125* (5), 1146-53.
- Berndt, A.; Miller S.; Williams O.; Le D.D.; Houseman B.T.; Pacold, J.I.; Gorrec, F.; Hon, W.-C.; Liu, Y.; Rommel, C.; Gaillard, P.; Ruckle, T.; Schwarz, M.K.; Shokat, K.M.; Shaw, J.P.; Williams, R.L. The p110 $\delta$  structure: mechanisms for selectivity and potency of new PI(3)k inhibitors. *Nat.Chem.Biol.* **2010**, *6* (2), 117-124.
- Evarts, J.B.; Ulrich, R. G. Atropisomers of PI3K-inhibiting compounds. WO2012/040634.
- Somoza J. R.; Koditek D.; Villaseñor A. G.; Novikov N.; Wong M. H.; Liclican A.; Xing W.; Lagpagan L.; Wang R.; Shultz B. E.; Papalia G. A.; Samuel D.; Lad L.; McGrath M. E. Structural, Biochemical, and Biophysical Characterization of Idelalisib Binding to Phosphoinositide 3-Kinase  $\delta$ . *J. Biol. Chem.*, **2015**, *290* (13), 8439-8446.
- Winkler, D. G.; Faia K. L.; DiNitto J. P.; Ali J. A.; White K. F.; Brophy E. E.; Pink M. M.; Proctor J. L.; Lussier J.; Martin C. M.; Hoyt J. G.; Tillotson B.; Murphy E. L.; Lim A. R.; Thomas B. D.; Macdougall J. R.; Ren P.; Liu Y.; Li L.; Jessen K. A.; Fritz C. C.; Dunbar J. L.; Poter J. R.; Rommel C.; Palombella V. J.; Changelian P. S.; Kutok J. L. PI3K- $\delta$  and PI3K- $\gamma$  inhibitor by IPI-145 abrogates immune responses and suppresses activity in autoimmune and inflammatory disease models. *Chem. Biol.* **2013**, *20* (11), 1364-74.
- McGinnity, D. F.; Soars M. G.; Ubanowicz R. A. and Riley R. J. Evaluation of fresh and cryopreserved hepatocytes as in vitro drug metabolism tools for the prediction of metabolic clearance. *Drug Metab. Dispos.* **2004**, *32*, 1247-1253.
- Heller R.; Chang Q.; Ehrlich G.; Hsieh S. N.; Schoenwaelder S. M.; Kuhlencordt P. J.; Preissner K. T.; Hirsch E. and Wetzker R. Overlapping and distinct roles for PI3K $\beta$  and  $\gamma$  isoforms in S1P-induced migration of human and mouse endothelial cells. *Cardiovasc. Res.*, **2008**, *80*, 96-105.
- Dal Porto J. M.; Gauld S. B.; Merrel K. T.; Mills D.; Pugh-Bernard A. E.; Cambier J. B cell antigen receptor signaling 101. *Mol. Immunol.* **2004**, *41*(6-7), 599-613.
- Banker M. J.; Clark T. H.; Williams J. A. Development and validation of 96Well Equilibrium dialysis apparatus for measuring plasma protein binding. *J. Pharm. Sci.*, **2003**, *92*(5), 967-974.
- Wohnsland F.; Faller B. High-throughput permeability pH profile and high-throughput alkane/water log P with artificial membranes. *J. Med. Chem.* **2001**, *44* (6), 923-30.
- Soond, D. R.; Slack, E. C. M.; Garden O. A.; Patton D. T.; Okkenhaug K. Does the PI3K pathway promote or antagonize regulatory T cell development and function? *Front. Immunol.* **2012**, *3*, 244.



**LAS191954**

PI3K $\delta$  IC<sub>50</sub> = 2.6 nM

M-CSF p-Akt IC<sub>50</sub> = 7.8 nM

% Metabolism (R / H) = 20 / 16

PK i.v. t<sub>1/2</sub> (R / D) = 3.1 h / 10.2 h